MEASUREMENT SCIENCE REVIEW

I-cored Coil Probe Located Above a Conductive Plate with a Surface Hole

Grzegorz Tytko, Leszek Dziczkowski

Institute of Electronics, Faculty of Automatic Control, Electronics and Computer Science, The Silesian University of Technology, Akademicka 16, 44-100, Gliwice, Poland, grzegorz.tytko@polsl.pl

This work presents an axially symmetric mathematical model of an I-cored coil placed over a two-layered conductive material with a cylindrical surface hole. The problem was divided into regions for which the magnetic vector potential of a filamentary coil was established applying the truncated region eigenfunction expansion method. Then the final formula was developed to calculate impedance changes for a cylindrical coil with reference to both the air and to a material with no hole. The influence of a surface flaw in the conductive material on the components of coil impedance was examined. Calculations were made in Matlab for a hole with various radii and the results thereof were verified with the finite element method in COMSOL Multiphysics package. Very good consistency was achieved in all cases.

Keywords: Nondestructive testing, eddy current, coil impedance, calculation, modeling, truncated region eigenfunction expansion.

1. Introduction

Eddy current testing is used in many industries to detect defects in conductive materials. In view of a minor penetration depth of eddy currents to the workpiece, the highest effectiveness is achieved for shallow flaws existing in non-ferromagnetic materials. Such flaws may occur both during the production process and because of material cracking or corrosion.

The solution to the problem of an air-cored coil located over the conductive material with a flaw was achieved for the hole in a plate [1], surface hole in a half-space [2]-[3], slot in a plate [4], and a plate with two flaws [5]. These studies were performed using the truncated region eigenfunction expansion (TREE) method, which was also applied for derivation of mathematical models of a planar spiral coil [6], an I-cored coil [7]-[8], a pot core coil [9], and a grating eddy current displacement sensor (GECDS) [10]. The examinations are usually conducted for coils wound around a core since such models feature a much higher sensitivity. The instruments used by the authors included also probes designed as I-cored coils with an air gap situated along the core axis (Fig.1.), which is described in [11]. This paper presents a mathematical model of such an I-cored coil placed over a two-layered conductive material with a cylindrical surface hole.

The rectangular cross-section coil is shown in Fig.2. The solution domain was limited to the value of parameter b, while maintaining the continuity of a magnetic vector potential. At the same time, satisfying the boundary condition, $A_\varphi (r, z) = 0$ for $r = 0$ and $r = b$ was ensured. During the analysis a filamentary coil was used, for which expressions that describe the magnetic vector potential were derived. Closed-form expressions for the change of I-cored coil impedance were obtained both in relation to the air as well as to the material with no hole. The results achieved using the TREE method were verified with the finite element method (FEM), which showed a very good agreement.
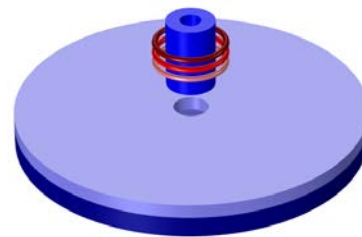
Fig.1. I-cored coil with a circular air gap inside the core column located above a conductive material with a surface hole.

2. Solution

At first, the analysis included a filamentary coil with a core located over a two-layer conductive material with a hole, which is presented in Fig.3. The axially symmetric system was divided into 6 regions. For each region, a magnetic vector potential was obtained, which was written using the matrix notation.

Fig.2. Rectangular cross-sectional coil located above a two-layered conductive plate with a hole.

Fig.3. Filamentary coil located above a two-layered conductive plate with a hole.

$$A_1(r,z) = J_1(\mathbf{q^T} r)\, \mathbf{q}^{-1} e^{-\mathbf{q}z} \mathbf{C}_1 \qquad (1)$$

$$A_2(r,z) = \begin{array}{ll} J_1(\mathbf{m^T} r) & 0 \le r \le a_1 \\ L_1(\mathbf{m^T} r)\, \mathbf{m}^{-1}(e^{-\mathbf{m}z}\mathbf{C}_2 - e^{\mathbf{m}z}\mathbf{B}_2) & a_1 \le r \le a_2 \\ L_1'(\mathbf{m^T} r) & a_2 \le r \le b \end{array} \qquad (2)$$

$$A_3(r,z) = \begin{array}{ll} J_1(\mathbf{m^T} r) & 0 \le r \le a_1 \\ L_1(\mathbf{m^T} r)\, \mathbf{m}^{-1}(e^{-\mathbf{m}z}\mathbf{C}_3 - e^{\mathbf{m}z}\mathbf{B}_3) & a_1 \le r \le a_2 \\ L_1'(\mathbf{m^T} r) & a_2 \le r \le b \end{array} \qquad (3)$$

$$A_4(r,z) = J_1(\mathbf{q^T} r)\, \mathbf{q}^{-1}(e^{-\mathbf{q}z}\mathbf{C}_4 - e^{\mathbf{q}z}\mathbf{B}_4) \qquad (4)$$

$$A_5(r,z) = \begin{array}{ll} J_1(\mathbf{u^T} r) R_1(\mathbf{v}\,g) & 0 \le r \le g \\ R_1(\mathbf{v^T} r) J_1(\mathbf{u}\,g) & g \le r \le b \end{array} \mathbf{u}^{-1}(e^{-\mathbf{u}z}\mathbf{C}_5 - e^{\mathbf{u}z}\mathbf{B}_5) \qquad (5)$$

$$A_6(r,z) = J_1(\mathbf{q^T} r)\, \mathbf{s}_6^{-1}(e^{-\mathbf{s}_6 z}\mathbf{C}_6 - e^{\mathbf{s}_6 z}\mathbf{B}_6) \qquad (6)$$

$$A_7(r,z) = -J_1(\mathbf{q^T} r)\, \mathbf{q}^{-1} e^{\mathbf{q}z}\mathbf{B}_7 \qquad (7)$$

where

$$\mathbf{u} = \sqrt{\mathbf{v}^2 + j\omega\mu_5\mu_0\sigma_5} \qquad (8)$$

$$\mathbf{s}_6 = \sqrt{\mathbf{q}^2 + j\omega\mu_6\mu_0\sigma_6} \qquad (9)$$

$J_1(\mathbf{q^T} r),\ L_1(\mathbf{q^T} r),\ L_1'(\mathbf{q^T} r),\ J_1(\mathbf{u^T} r), R_1(\mathbf{v^T} r)$ – row vectors

$\mathbf{q}, \mathbf{m}, \mathbf{u}, \mathbf{v}, \mathbf{s}_6, e^{\pm\mathbf{q}z}, e^{\pm\mathbf{m}z}, e^{\pm\mathbf{u}z}, e^{\pm\mathbf{s}_6 z}$ – diagonal matrices

$\mathbf{C}_i, \mathbf{B}_i$ – column vectors of unknown coefficients

Discrete eigenvalues q_i and m_i are the positive roots of the equations (10) and (11). Such values are not present in region 5 that has a hole, so they are calculated in the same way as in the case of an I-cored coil located over the material without a hole [9].

$$J_1(q_i b) = 0 \qquad i = 0,1,2...Ns \qquad (10)$$

$$L_1'(m_i b) = 0 \qquad i = 0,1,2...Ns \qquad (11)$$

where

$$L_1'(m_i r) = B_{2F}'\, J_1(m_i r) + C_{2F}'\, Y_1(m_i r) \qquad (12)$$

$$C_{2F}' = \frac{\pi}{2} m_i a_2 \left[\frac{J_1(m_i a_2) L_0(m_i a_2)}{\mu_f} - J_0(m_i a_2) L_1(m_i a_2) \right] \qquad (13)$$

$$B_{2F}' = -\frac{\pi}{2} m_i a_2 \left[\frac{Y_1(m_i a_2) L_0(m_i a_2)}{\mu_f} - Y_0(m_i a_2) L_1(m_i a_2) \right] \qquad (14)$$

$$L_n(m_i r) = B_{2F}\, J_n(m_i r) + C_{2F}\, Y_n(m_i r) \qquad (15)$$

$$C_{2F} = \frac{\pi}{2} m_i a_1 (\mu_f - 1) J_0(m_i a_1) J_1(m_i a_1) \qquad (16)$$

$$B_{2F} = \frac{\pi}{2} m_i a_1 [\mu_f J_0(m_i a_1) Y_1(m_i a_1) - J_1(m_i a_1) Y_0(m_i a_1)] \qquad (17)$$

Region 5 of the analyzed problem consists of two sub-regions: air space ($0 \ge r \ge g$) and a conductive material ($g \ge r \ge b$). The magnetic vector potential for those sub-regions may be expressed in a general form as:

$$A_I = A_E J_1(u_i r) R_1(v_i g) \qquad 0 \le r \le g \qquad (18)$$

$$A_{II} = A_E R_1(v_i\, r)\, J_1(u_i\, g) \qquad g \le r \le b \qquad (19)$$

where

$$R_n(v_i\, x) = Y_1(v_i\, b)\, J_n(v_i\, x) + J_1(v_i\, b)\, Y_n(v_i\, x) \qquad (20)$$

Equation (21) was obtained using the interface condition $(1/r)[\partial(rA)/\partial r] = 0$ in the radial direction for $r = g$ [7].

$$u_i\, R_1(v_i\, g)\, J_0(u_i\, g) = \frac{1}{\mu_5} v_i\, J_1(u_i\, g)\, R_0(v_i\, g) \qquad (21)$$

Calculation of u_i and v_i eigenvalues is reduced to finding complex roots of the equation (21). Using numerical procedures, such as FindRoot() in Mathematica or fzero() in Matlab, requires providing initial values around which the roots are located. Such initial values may be taken as u_i values obtained upon the assumption that region 5 consists only of a conductive material or only of air. In the first case, when $g = 0$, we obtain $u_i = s_{5i}$, and in the second case $g = b$ and, in consequence, $u_i = q_i$ [7]. Unfortunately, this method may lead to omission of some roots. Higher effectiveness is achieved with the Newton-Raphson technique. However, in some cases even applying a very low increase in the argument does not ensure finding all the roots. The solution to this problem may be found by using more complex algorithms [10]-[11] which, upon appropriate selection of parameters, allow to properly derive all u_i, v_i values.

The unknown coefficients $\mathbf{C}_i$, $\mathbf{B}_i$ occurring in (1)-(7) were calculated using, for mutually neighboring regions of the problem, the following continuity conditions B_r and H_z.

$$A_i(r, z) = A_{i+1}(r, z) \qquad (22)$$

$$\frac{1}{\mu_i}\frac{\partial A_i}{\partial z} - \frac{1}{\mu_{i+1}}\frac{\partial A_{i+1}}{\partial z} = -\mu_0 I \delta(r - r_0) \qquad (23)$$

where
$\mu_0 I \delta(r - r_0)$ – current density

The solution to the system of interface equations obtained in this way was written down as:

$$\begin{matrix}\mathbf{B}_{47} \\ \mathbf{C}_{47}\end{matrix} = \mp \frac{1}{2} e^{\pm \mathbf{q}\, l_1}[(\mathbf{q}\mathbf{u}^{-1}\mathbf{K} \mp \mathbf{V})e^{\mathbf{u}\, l_1}\mathbf{C}_{57} - (\mathbf{q}\mathbf{u}^{-1}\mathbf{K} \pm \mathbf{V})e^{-\mathbf{u}\, l_1}\mathbf{B}_{57}]$$

$$(24)$$

$$\begin{matrix}\mathbf{B}_{57} \\ \mathbf{C}_{57}\end{matrix} = \mp \frac{1}{2} e^{\pm \mathbf{u}\, l_2}[(\mathbf{s}_6^{-1}\mathbf{u}\,\mathbf{K}^{-1} \mp \frac{1}{\mu_6}\mathbf{V}^{-1})e^{\mathbf{s}_6\, l_2}\mathbf{C}_{67}$$
$$-\, (\mathbf{s}_6^{-1}\mathbf{u}\,\mathbf{K}^{-1} \pm \frac{1}{\mu_6}\mathbf{V}^{-1})e^{-\mathbf{s}_6\, l_2}\mathbf{B}_{67}] \qquad (25)$$

$$\begin{matrix}\mathbf{B}_{67} \\ \mathbf{C}_{67}\end{matrix} = \frac{1}{2} e^{\pm \mathbf{s}_6\, l_3} e^{-\mathbf{q}\, l_3}(\mu_6 \pm \mathbf{s}_6\mathbf{q}^{-1}) \qquad (26)$$

where

$$\mathbf{K} = R_1(\mathbf{v}\, g)\int_0^g J_0(\mathbf{q}\, r)\, J_0(\mathbf{u}^\mathrm{T} r)\, r\, dr$$
$$+\, J_1(\mathbf{u}\, g)\int_g^b J_0(\mathbf{q}\, r)\, R_0(\mathbf{v}^\mathrm{T}\, r)\, r\, dr \qquad (27)$$

$$\mathbf{V} = R_1(\mathbf{v}\, g)\int_0^g J_1(\mathbf{q}\, r)\, J_1(\mathbf{u}^\mathrm{T} r)\, r\, dr$$
$$+\, \frac{1}{\mu_{r5}} J_1(\mathbf{u}\, g)\int_g^b J_1(\mathbf{q}\, r)\, R_1(\mathbf{v}^\mathrm{T}\, r)\, r\, dr \qquad (28)$$

The magnetic vector potential for each region of the problem with the coil presented in Fig.2. may be calculated using the equation:

$$A(r, z) = \int_{r_1}^{r_2}\int_{h_1}^{h_2} A_{filamentary}(r, z, r_0, h_0)\, dr_0\, dh_0 \qquad (29)$$

After integrating the magnetic vector potential of region 2-3 over the coil's cross section, an expression for the impedance of an I-cored coil placed over the two-layered conductive plate with a surface hole was obtained.

$$Z = \frac{j\omega\,\pi\mu_0 N^2}{[(r_2 - r_1)(h_2 - h_1)]^2}\chi(\mathbf{m}^\mathrm{T} r_1, \mathbf{m}^\mathrm{T} r_2)\mathbf{m}^{-4}\{2(h_2 - h_1)\mathbf{m}$$
$$+\, e^{\mathbf{m}(h_1 - h_2)} - e^{\mathbf{m}(h_2 - h_1)} - \mathbf{M}\mathbf{N}^{-1}[(\mathbf{T} + \mathbf{U})\, e^{\mathbf{m}\, d}(e^{-\mathbf{m}\, h_1} - e^{-\mathbf{m}\, h_2})$$
$$-\, (\mathbf{T} - \mathbf{U})\, e^{-\mathbf{m}\, d}\times(e^{\mathbf{m}\, h_2} - e^{\mathbf{m}\, h_1})]\}\, \mathbf{m}^{-3}\mathbf{D}^{-1}\chi(\mathbf{m}\, r_1, \mathbf{m}\, r_2)$$

$$(30)$$

where

$$\chi(\mathbf{m}\, r_1, \mathbf{m}\, r_2) = \int_{\mathbf{m}\, r_1}^{\mathbf{m}\, r_2} r\, L_1(\mathbf{m}\, r)\, dr \qquad (31)$$

$$\mathbf{D} = \int_0^{a_1} J_0(\mathbf{m}\, r)\, J_0(\mathbf{m}^\mathrm{T} r)\, r\, dr$$
$$+\, \frac{1}{\mu_f}\int_{a_1}^{a_2} L_0(\mathbf{m}\, r)\, L_0(\mathbf{m}^\mathrm{T} r)\, r\, dr + \int_{a_2}^b L_0^{'}(\mathbf{m}\, r)\, L_0^{'}(\mathbf{m}^\mathrm{T} r)\, r\, dr \qquad (32)$$

$$\mathbf{T} = \int_0^{a_1} J_0(\mathbf{q}\, r)\, J_0(\mathbf{m}^\mathrm{T} r)\, r\, dr$$
$$+\, \int_{a_1}^{a_2} J_0(\mathbf{q}\, r)\, L_0(\mathbf{m}^\mathrm{T} r)\, r\, dr + \int_{a_2}^b J_0(\mathbf{q}\, r)\, L_0^{'}(\mathbf{m}^\mathrm{T} r)\, r\, dr \qquad (33)$$

$$\mathbf{U} = \int_{0}^{a_1} J_1(\mathbf{q}\, r) J_1(\mathbf{m}^{\mathbf{T}} r)\, r\, dr$$
$$+ \frac{1}{\mu_f} \int_{a_1}^{a_2} J_1(\mathbf{q}\, r) L_1(\mathbf{m}^{\mathbf{T}} r)\, r\, dr + \int_{a_2}^{b} J_1(\mathbf{q}\, r) L_1'(\mathbf{m}^{\mathbf{T}} r)\, r\, dr$$

$$(34)$$

$$\mathbf{M} = (e^{-\mathbf{m}\, h_1} - e^{\mathbf{m}\, h_2})[(\mathbf{U}^{-1} + \mathbf{T}^{-1})\, \mathbf{C}_{47} + (\mathbf{U}^{-1} - \mathbf{T}^{-1})\, \mathbf{B}_{47}]$$
$$- (e^{-\mathbf{m}\, h_2} - e^{\mathbf{m}\, h_1})[(\mathbf{U}^{-1} - \mathbf{T}^{-1})\, \mathbf{C}_{47} + (\mathbf{U}^{-1} + \mathbf{T}^{-1})\, \mathbf{B}_{47}]$$

$$(35)$$

$$\mathbf{N} = (\mathbf{T} + \mathbf{U})\, e^{\mathbf{m}\, d}[(\mathbf{U}^{-1} - \mathbf{T}^{-1})\, \mathbf{C}_{47} + (\mathbf{U}^{-1} + \mathbf{T}^{-1})\, \mathbf{B}_{47}]$$
$$- (\mathbf{T} - \mathbf{U})\, e^{-\mathbf{m}\, d}[(\mathbf{U}^{-1} + \mathbf{T}^{-1})\, \mathbf{C}_{47} + (\mathbf{U}^{-1} - \mathbf{T}^{-1})\, \mathbf{B}_{47}]$$

$$(36)$$

The impedance of the coil $Z_0 = R_0 + jX_0$ located in the space with no conductive material was calculated after substituting $\sigma_5 = \sigma_6 = 0$ in (30). Then, by subtracting the Z_0 value obtained in this way from (30), the change of the coil impedance ΔZ was obtained. It was caused by placing the coil over the conductive material with a hole.

$$\Delta Z = Z - Z_0 \qquad (37)$$

For applications related to flaw detection (defectoscopy), the change of impedance calculated in relation to the workpiece with no hole proves to be highly significant. The value $\Delta Z_h = \Delta R_h + j\Delta X_h$ obtained in this manner presents the situation where the impedance of the coil placed over the surface of the workpiece has been changed due to the occurrence of a hole.

$$\Delta Z_h = \left| Z - Z_{without\ hole} \right| \qquad (38)$$

The impedance of the I-cored coil located over the conductive plate with no hole was calculated by substituting $g = 0$ in (30). In such a case $\mathbf{v} = \mathbf{q}$, $\mathbf{K} = \mathbf{E}$, $\mathbf{V} = \mathbf{E}/\mu_5$ and coefficients $\mathbf{C}_{57}$, $\mathbf{B}_{57}$ were reduced to the following form:

$$\begin{aligned} \mathbf{B}_{57} \\ \mathbf{C}_{57} \end{aligned} = \mp \frac{1}{2} e^{\pm \mathbf{s}_5\, l_2} [(\mathbf{s}_5 \mathbf{s}_6^{-1} \mp \frac{\mu_5}{\mu_6} \mathbf{V}^{-1}) e^{\mathbf{s}_6\, l_2} \mathbf{C}_{67}$$
$$- (\mathbf{s}_5 \mathbf{s}_6^{-1} \pm \frac{\mu_5}{\mu_6} \mathbf{V}^{-1}) e^{-\mathbf{s}_6\, l_2} \mathbf{B}_{67}] \qquad (39)$$

3. RESULTS AND DISCUSSION

The parameters of the coil and the conductive material used in calculations are presented in Table 1. The inductance L_0 was respectively equal to: 3.39 mH for the I-cored coil and 1.89 mH for the air-cored coil. The coil impedance was calculated from (41) while assuming the number of summation terms $Ns = 50$ and the domain radius $b = 12\, r_2$, which corresponds to the value of 54 mm. For the

inversion of matrices as well as calculating additional discrete eigenvalues m_i, inv() and fzero() functions available in Matlab were used. The complex values u_i were computed using the approach based on Cauchy's theorem, which is described in detail in [12]. Pursuant to this method the solution domain was divided into rectangles so that each one of them contained not more than one root. Such an approach made it possible to avoid omission of some u_i values.

Table 1. Parameters of the coil, core, and plate used in calculations.

Inner core radius	a_1	0.5 mm
Outer core radius	a_2	1.5 mm
Length	d	5 mm
Inner coil radius	r_1	1.8 mm
Outer coil radius	r_2	4.5 mm
Offset	h_1	0.1 mm
Parameter	h_2	4 mm
Number of turns	N	700
Liftoff	l_1	0.1 mm
Parameter	l_2	2.1 mm
Parameter	l_3	22.1 mm
Relative permeability	μ_f	2000
Relative permeability	μ_5, μ_6	1
Conductivity	σ_5, σ_6	10 MS m^{-1}
Radius of the domain	b	54 mm
Radius of the hole	g	2.5 mm

The results obtained from Matlab calculations were then verified by means of the finite elements method in COMSOL Multiphysics package. The mesh applied for computations was made up of about 31000 triangular elements and 800 edge elements. The highest density of mesh elements was used around the hole edge and under the coil winding. The calculations for changes ΔZ and ΔZ_h of coil impedance were performed for the range of frequencies from 100 Hz to 100 kHz. All results have been normalized in relation to the reactance X_0 and are presented in Fig.4. and Fig.5. The values for changes of the coil impedance components calculated with use of the proposed mathematical model were only different from the results obtained with COMSOL Multiphysics. In the case of resistance changes, such a difference did not exceed 1.21 %, and for changes of reactance, it was not higher than 0.62 %.

Fig.6. presents the coil resistance changes normalized in relation to reactance X_0 after placing the coil over the conductive material with radius varying from $g = 0$ to $g = 10$ mm. Further increase of the radius g led to only insignificant variation of the coil resistance since the highest density of eddy currents occurred in such a part of the conductive material which is located under the winding. The occurrence of the flaw has a far higher influence on resistance than on reactance. For example, when the frequency was $f = 1$ kHz and a surface hole with the radius of $g = 10$ mm was made in the workpiece, the coil reactance changed only by 2 % but its resistance was amended by as much as 184 %.
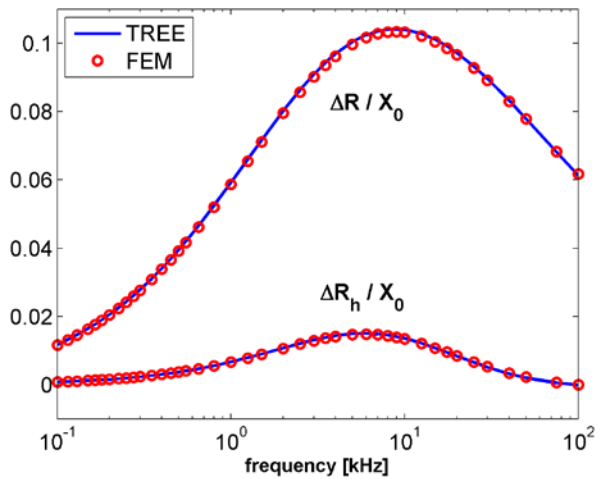
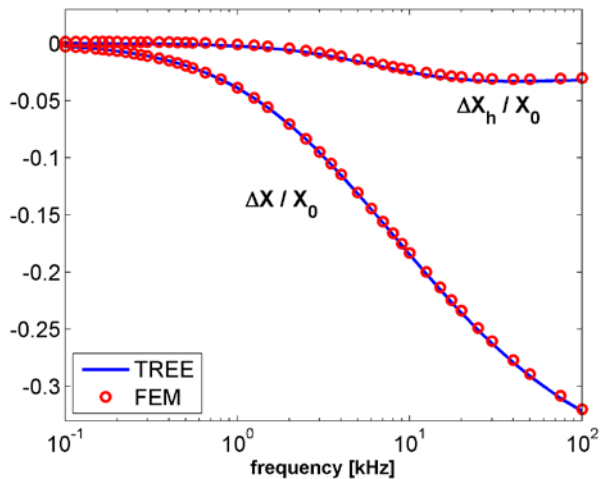Fig.4. Real part of the normalized impedance changes as a function of frequency.

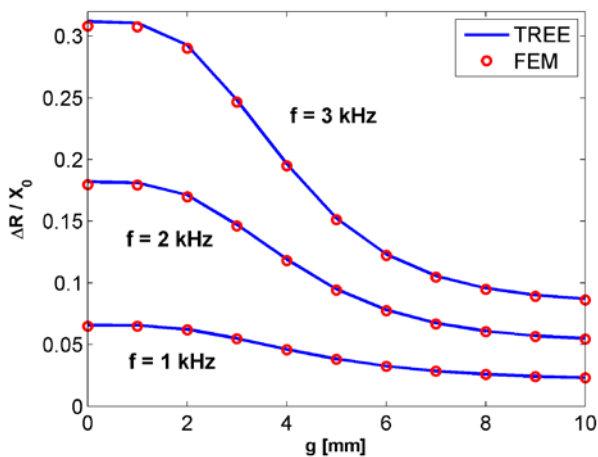Fig.5. Imaginary part of the normalized impedance changes as a function of frequency.

Fig.6. Real part of the normalized impedance changes as a function of the hole radius.

4. CONCLUSION

The axially symmetric mathematical model proposed herein makes it possible to calculate the impedance of an I-cored coil placed over a two-layered conductive plate with a cylindrical surface hole. The final formulas obtained with the use of the TREE method can be implemented in any mathematical software, such as Mathematica or Matlab. Calculations can be made for any size of a hole, even while changing its radius (g) and depth (l_2-l_1). Values of the coil impedance components obtained with the use of proposed solution were verified with the application of the finite elements method. The difference obtained did not exceed 1.21 % for resistance and 0.62 % for reactance within the range of frequency from 100 Hz to 100 kHz. The performed verification of results proved that the mathematical model presented in this work can be used as a substitute for numerical solutions that utilize the finite elements method.

REFERENCES

[1] Theodoulidis, T.P., Bowler, J.R. (2004). The truncated region eigenfunction expansion method for the solution of boundary value problems in eddy current non-destructive evaluation. *Review of Progress in Quantitative Nondestructive Evaluation*, 24A, 403–408.

[2] Kolyshkin, A. (2013). Solution of direct eddy current problems with cylindrical symmetry. In *Proceedings of the International Conference on Application of Contemporary Non-destructive Testing in Engineering*, 4–6 September 2013. Portoroz, Ljubljana, Slovenia: University of Ljubljana, 347–351.

[3] Koliskina, V. (2014). Semi-analytical solution of an eddy current problem for a conducting medium with a surface flaw. *International Journal of Mathematical Models and Methods in Applied Sciences*, 8, 473-480.

[4] Theodoulidis, T.P., Bowler, J.R. (2005). Eddy-current interaction of a long coil with a slot in a conductive plate. *IEEE Transactions on Magnetics*, 41 (4), 1238–1247.

[5] Koliskina, V., Kolyshkin, A. (2015). Mathematical model for eddy current testing of metal plates with two cylindrical flaws. In *IEEE 15th International Conference on Environment and Electrical Engineering (EEEIC)*, 10-13 June 2015, 374-377.

[6] Hao, K., Huang, S., Zhao, W., Wang, S., Dong, J. (2011). Analytical modelling and calculation of pulsed magnetic field and input impedance for EMATs with planar spiral coils. *NDT&E International*, 44 (3), 274–280.

[7] Theodoulidis, T.P., Kriezis, E.E. (2006). *Eddy Current Canonical Problems (With Applications to Nondestructive Evaluation)*. Duluth (Georgia), USA: Tech Science Press.

[8] Lu, Y., Bowler, J.R, Theodoulidis, T.P. (2012). An analytical model of a ferrite-cored inductor used as an eddy current probe. *Journal of Applied Physics*, 111 (10), 103907.

[9]   Tytko, G. Dziczkowski, L. (2015). E-cored coil with a circular air gap inside the core column used in eddy current testing. *IEEE Transactions on Magnetics*, 51 (9), 6201804.

[10]   Chunfeng, L., Wei, T., Huaming, L., Yingying, J., Hui, Z. (2015). Analytical modeling for the grating eddy current displacement sensors. *Measurement Science Review*, 15 (1), 44-51.

[11]   Tytko, G., Dziczkowski, L. (2017). An analytical model of an I-cored coil with a circular air gap. *IEEE Transactions on Magnetics*, 53 (4), 6201104.

[12]   Delves, L.M., Lyness, J.N. (1967). A numerical method for locating the zeros of an analytic function. *Mathematics of Computation*, 21 (100), 543–560.

[13]   Dellnitz, M., Schütze, O., Zheng, Q. (2002). Locating all the zeros of an analytic function in one complex variable. *Journal of Computational and Applied Mathematics*, 138 (2), 325-333.